CONSTRAINING THE DISTRIBUTION OF DARK MATTER IN INNER GALAXY WITH INDIRECT DETECTION SIGNAL: THE CASE OF TENTATIVE 130 GEV γ-RAY LINE

Rui-Zhi Yang[1,2], Lei Feng[1], Xiang Li[1,2] and Yi-Zhong Fan[1,*]

Draft version May 1, 2013

ABSTRACT

The dark matter distribution in the very inner region of our Galaxy is still in debate. In the N-body simulations a cuspy dark matter halo density profile is favored. Several dissipative baryonic processes however are found to be able to significantly flatten dark matter distribution and a cored dark matter halo density profile is possible. The baryons dominate the gravitational potential in the inner Galaxy, hence a direct constrain on the abundance of the dark matter particles is rather challenging. Recently, a few groups have identified a tentative 130 GeV line signal in the Galactic center, which could be interpreted as the signal of the dark matter annihilation. With current 130 GeV line data and adopting the generalized Navarro-Frenk-White profile of the dark matter halo, for local dark matter density $\rho_0 = 0.4$ GeV cm^{-3} and $r_{\rm s} = 20$ kpc we obtain a 95% confidence level lower (upper) limit on the inner slope of dark matter density distribution $\alpha = 1.06$ (the cross section of dark matter annihilation into gamma-rays $\langle \sigma v \rangle_{\chi\chi \to \gamma\gamma} = 1.3 \times 10^{-27}$ cm^3 s^{-1}). Such a slope is consistent with the results of some N-body simulations, and if the signal is due to dark matter, suggests that baryonic processes may be unimportant.

Subject headings: Dark matter$-$Gamma Rays: general$-$galaxies: structure

1. INTRODUCTION

In the leading cold dark matter (CDM) model, structure forms hierarchically bottom-up, with DM collapsing first into small halos, which then accrete normal matter, merge and eventually give rise to larger halos. Galaxies are thought to form out of gas which cools and collapses to the centers of these DM haloes (e.g., White & Rees 1978). As shown in the high-resolution N-body simulations, the density profiles of CDM halos can be reasonably well described by an universal form, independent of the halo mass, and the cuspy density profiles such as Navarro-Frenk-White (NFW, Navarro et al. 1997) and Einasto (Einasto 1965) are found to be favored. The effect of the baryons ignored in most previous simulations, however, are still to be figured out. One possibility is the so-called adiabatic contraction, i.e., when the Galaxy formed and the baryons contracted towards the centre, dark matter particles are pulled inward and their central density increases (e.g., Blumenthal et al. 1986; Gnedin et al. 2004). The resulting DM profile of the galaxies is expected to be more cuspy. Contrary to adiabatic contraction, other baryonic processes, such as the gas bulk motions, possibly supernova-induced in regions of high star formation activity, and the subsequent energy loss of gas clouds due to dynamical friction, can transfer energy to the central dark matter component or/and induce substantial gravitational potential fluctuations and finally give rise to a subsequent reduction in the central dark matter density (e.g., Navarro et al. 1996; Mo & Mao 2004; El-Zant et al. 2001; Mashchenko et al. 2006;

Ogiya & Mori 2011; Maccio et al. 2012; Pontzen & Governato 2012). The resulting DM profile of the Galaxies is likely cored.

As shown in the recent high-resolution cosmological hydrodynamical simulations performed by Maccio et al. (2012; see Fig.1 therein) and by Pontzen & Governato (2012; see Fig.5 therein), with and without the effects of dissipative baryonic processes the inner distribution of dark matter in Milky-Way-like objects are indeed rather different. Nevertheless these dark matter profiles only represent the mean of all simulated halos for a given mass at a given redshift. The scatter with respect to these mean values arises plausibly due to the different halo formation histories and due to the evolution of the expanding Universe (e.g., Navarro et al. 2010; Wu et al. 2013). The average values may be unable to describe accurately the DM halo of the Milky Way since its formation and evolution may not follow a prototypical spiral galaxy. In view of such uncertainties, observational data is highly needed to reliably constrain the inner structure of the Milky Way DM halo. However, current microlensing and dynamical data can only rule out some extremely cuspy density profiles (Iocco et al. 2011) since in inner Galaxy, the gravitational potential is dominated by the normal matter rather than the dark matter. It is well established that the prospect of detecting the products of dark matter particle annihilation is critically sensitive to the structure of the Milky Way DM halo. Moreover, a robust estimate of the cross section of dark matter particles annihilating into normal matter (photons, electrons/positrons and so on) is not possible unless the DM halo profile has been reasonably well determined. In turn, indirect DM gamma-ray searches can be used to study the distribution of DM in the innermost regions of the Milky Way halo as long as a positive signal (in particular an unambiguous gamma-ray line) has been identified. In this work, we adopt the

[1] Key Laboratory of Dark Matter and Space Astronomy, Purple Mountain Observatory, Chinese Academy of Sciences, Nanjing 210008, China
[2] Graduate University of Chinese Academy of Sciences, Beijing, 100012, China
[*] To whom the correspondence should be sent (email: yzfan@pmo.ac.cn).

hypothesis that the Galactic ~ 130 GeV line signal identified in the publicly available Fermi-LAT data firstly by Bringman et al. (2012) and Weniger (2012) originated from the annihilation of dark matter. Under this hypothesis, we examine which dark matter density profiles are consistent with the signal, and then discuss the implication.

2. CONSTRAINING THE DARK MATTER DENSITY PROFILE AND $\langle \sigma V \rangle_{\chi\chi\to\gamma\gamma}$ WITH THE 130 GEV LINE SIGNAL

2.1. The 130 GeV line signal

High energy γ-ray line is of greatest interest in looking for the signal of dark matter annihilation. After analyzing the publicly available Fermi-LAT γ-ray data, Bringman et al. (2012) and Weniger (2012) found possible evidence for a monochromatic γ-ray line with energy ~ 130 GeV. Later independent analyses confirmed such an excess. The center of the most prominent signal region is around the Galactic centre Sgr A* with an offset $\geq 1.2°$ (Tempel et al. 2012; Su & Finkbeiner 2012), which has been thought to be at odds with the DM origin. However, within the DM annihilation scenario such an offset can be interpreted by the limited statistics of the current $\gamma-$ray line signal consisting of only ~ 14 photons (Yang et al. 2012). Furthermore, it is interesting to note that there is a small wiggle in the electron spectrum of PAMELA/Fermi-LAT at energies ~ 100 GeV, which may be interpreted as being consistent with the 130 GeV line signal (Feng et al. 2013).

With a typical cuspy DM density profile such as Navarro-Frenk-White (NFW, Navarro et al. (1997)) and Einasto (1965), annihilation cross section $\langle \sigma v \rangle_{\chi\chi\to\gamma\gamma} \sim 2 - 5 \times 10^{-27} \mathrm{cm}^3 \mathrm{~s}^{-1}$ is needed to produce the signal data (Weniger 2012; Tempel et al. 2012), which however is larger than the upper limit ($\sim 10^{-27} \mathrm{cm}^3 \mathrm{~s}^{-1}$) set by the non-detection of 130 GeV line in other regions by a factor of quite a few. This puzzle has been taken to be a piece of evidence against the dark matter origin of the 130 GeV line in the Milky Way center (e.g., Huang et al. 2012). As already mentioned in Sec. 1, in the Galactic center the DM density profile is rather uncertain, it is thus *not* confidential to refute the dark matter model just based on the tension between the values or upper-limits of $\langle \sigma v \rangle_{\chi\chi\to\gamma\gamma}$ inferred in different regions.

In principle, one may be able to find an ideal region to reliably evaluate $\langle \sigma v \rangle_{\chi\chi\to\gamma\gamma}$. In such a region the following conditions should be met, including (i) The dark matter density distribution is reasonably determined by astrophysical observations; (ii) The signal-to-noise is relatively high; (iii) The contribution of the DM substructure is expected to be not dominated. For the Milky Way, the dynamical data plays a role in constraining the dark matter distribution for $r > 3$ kpc, where r is the distance to the Galactic center (e.g., Sofue 2012). Observationally there is still no strong evidence for the existence of abundant substructures of the Milky Way dark matter halo. The N-body simulation Aquarius found out that abundant substructures of the Galaxies might present at $r > 20$ kpc (Springel et al. 2008). The contribution to the J-factor may be non-ignorable (i.e., the contribution is about the same as the smooth halo) any longer at $\psi \approx 30°$. Unless for the very cuspy dark matter halo, the

signal-to-noise is also acceptable in the region $\psi \gtrsim 30°$ (e.g., Bringman et al. 2012). In view of these facts, the region $\psi \in (20°, 40°)$ excluding $b \leq 10°$ may be a suitable region to constrain/measure $\langle \sigma v \rangle_{\chi\chi\to\gamma\gamma}$, where b is the Galactic latitude and ψ is the angle to the Galactic centre. As an unbiased constraint on the dark matter density profile, the data in other regions should be taken into account, too. It should also be mentioned that the dwarf galaxies are also ideal candidates to constrain the annihilation cross section of dark matter. Geringer-Sameth & Koushiappas (2012) performed a joint analysis of dwarf galaxy data and found that the upper limit on the annihilation cross section to a two-photon final state is $3.9^{+7.1}_{-3.7} \times 10^{-26} \mathrm{cm}^3 \mathrm{~s}^{-1}$ at 130 GeV (see also Huang et al. 2012), which is well above that needed to account for the signal identified in the Galactic center (see below).

2.2. Fermi LAT data Analysis

In last subsection we have suggested that $\psi \in (20°, 40°)$ excluding $b \leq 10°$ may be a suitable region to constrain/measure $\langle \sigma v \rangle_{\chi\chi\to\gamma\gamma}$. In reality, for a given dark matter density profile the intrinsic $\langle \sigma v \rangle_{\chi\chi\to\gamma\gamma}$ should be smaller than the values or upper limits inferred from any other regions. Currently the tentative $\gamma-$ray signal is present in a very compact region, hence we are only able to set an upper limit on $\langle \sigma v \rangle_{\chi\chi\to\gamma\gamma}$ and impose a constraint on the slope of the dark matter density profile.

For such a purpose, we analyze the publicly available Fermi-LAT data in several regions: including (a) $\psi \leq 2°$, which covers the most prominent signal region identified in Tempel et al. (2012); (b) the region $\psi \in (2°, 6°)$; (c) the region $\psi \in (6°, 10°)$;(d) the region $\psi \in (10°, 20°)$ excluding $b \leq 10°$; (e) the region $\psi \in (20°, 30°)$ excluding $b \leq 10°$;(f) the region $\psi \in (30°, 45°)$ excluding $b \leq 10°$; (g) the rest region $\psi \in (45°, 180°)$ excluding $b \leq 10°$. We take into account the data in the time interval from 4 August 2008 to 18 April 2012 (MET 239557417 - MET 356439845), with energies between 20 and 200 GeV. We used the standard LAT analysis software (v9r27p1)[4]. To reduce the effect of the Earth albedo background, time intervals when the Earth was appreciably in field-of-view (FoV), specifically when the center of the FoV was more than $52°$ from zenith, as well as time intervals when parts of the ROI were observed at zenith angles $> 100°$ were also excluded from the analysis. The spectral analysis was performed based on the P7v6 version of post-launch instrument response functions (IRFs). ULTRACLEAN dataset was selected to avoid the contamination from the charged particle. The spectra are shown in Fig.1.

To investigate the line signal at 130 GeV we use the unbinned analysis method which is similar to the one described in (Ackermann et al. 2012). It should be noted that in drawing fig.1 we binned the counts to different energy bins, which may introduce fake signal when the counts number is small. However, in fitting the data to derive the possible line signal or upper limits we use the unbinned analysis, say, the likelihood function was built by multiply the probability distribution function of each photons in the assuming model. This method can minimize the fake signal due to binning and take advantage of
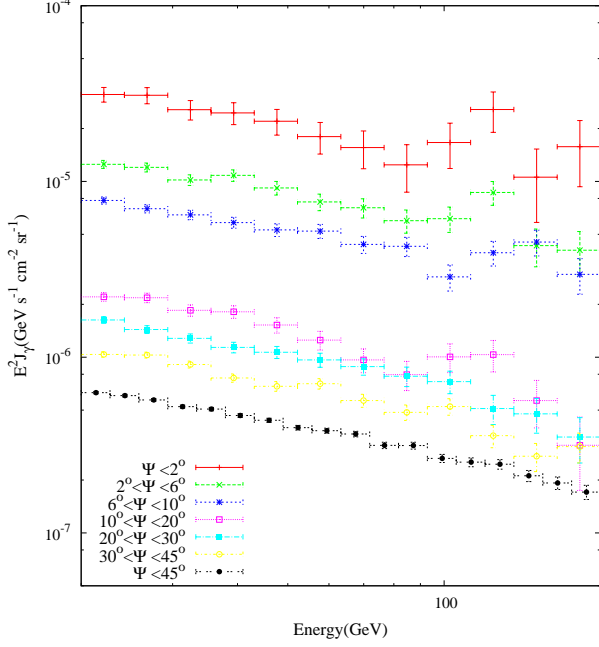
---

[4] http://fermi.gsfc.nasa.gov/ssc

Fig. 1.— The 20-200 GeV spectra of our Galaxy in seven regions described in the text (Please note that $b \leq 10^0$ is excluded for the last four regions). J_γ is the differential gamma ray flux.

the full information of the observed data. The likelihood is described as

$$\mathcal{L} = \prod_i f S(E_i) + (1-f)B(E_i), \qquad (1)$$

where $S(E_i)$ and $B(E_i)$ represent the signal and background function, respectively, both are normalized to 1, and i runs over all the photons; f is the signal fraction and has been set to be in the range $[-1, 1]$ for line signal search and $[0, 1]$ for getting upper limits; $B(E_i)$ takes the form

$$B(E_i) \sim E_i^{-\Gamma}\epsilon(E_i), \qquad (2)$$

where $\epsilon(E_i)$ is the exposure generated by the *gtexpcube2* routine. $S(E_i)$ is derived by convolving the energy dispersion function and exposure. Pyminuit [5] are used to find the maximum of the likelihood. The MINOS asymmetric error at the level $\Delta \ln \mathcal{L} = 1.35$ is adopted to get upper limit corresponding to a coverage probability of 95%. To see the possible systematics due to the different choice of the background spectrum, we redo the analysis by using two different background spectral template $B(E_i)$: (1) adding an exponential cutoff to the pure power law spectrum and leaving the cutoff energy to be free, say,

$$B(E_i) \sim E_i^{-\Gamma}exp(-E_i/E_{cut})\epsilon(E_i), \qquad (3)$$

(2) a log-parabola spectrum

$$B(E_i) \sim (\frac{E_i}{E_b})^{-(\alpha+\beta log(E_i/E_b))}\epsilon(E_i). \qquad (4)$$

We do not find significant improvement of the fitting, thus for simplicity we use the pure power law spectrum as our fiducial background spectral model.
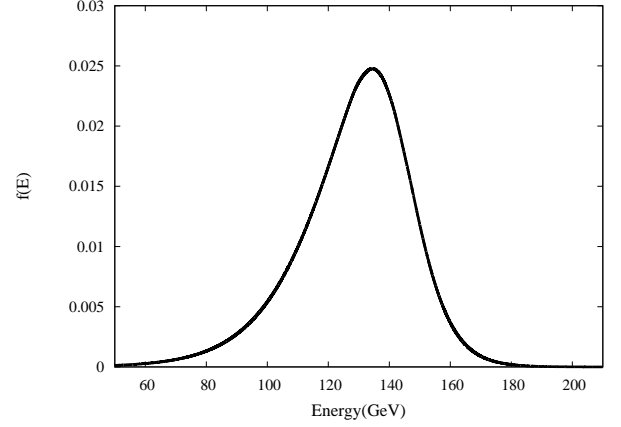
Fig. 2.— The energy dispersion used in our analysis. The form of energy dispersion is described in the text and has already been normalized.

The region we choose is all larger than several degrees, meanwhile, the angular resolution above 20 GeV is within 0.2 degree, which is much smaller than the size of the region of interest. Thus we neglect the point dispersion function(PSF) in the analysis. On the other hand, the energy dispersion is extremely important in the line searching process. In this work we focus on the tentative 130 GeV line, and adopt the energy dispersion at 130GeV with the form described on the website [6]. The P7ULTRACLEANV6 version of the instrument response functions(IRFs) is used and the final energy dispersion is averaged for different incidence angles. The derived energy dispersion used in the analysis is shown in Fig.2 and the signal flux (or upper limits) obtained in different regions are summarized in Tab.1.

TABLE 1
The signal flux as well as the 95% confidence level upper limits obtained in different regions. Please note that $b \leq 10^0$ is excluded for the last four regions.

Region	Position	Signal/upper limit (10^{-8} cm^{-2}s^{-1}sr^{-1})
a	$\psi \leq 2°$	3.8 ± 1.6
b	$\psi \in (2°, 6°)$	0.55
c	$\psi \in (6°, 10°)$	0.34
d	$\psi \in (10°, 20°)$	0.133
e	$\psi \in (20°, 30°)$	0.028
f	$\psi \in (30°, 45°)$	0.0084
g	$\psi \geq 45°$	0.0015

2.3. Constraints on $\langle\sigma v\rangle_{\chi\chi\to\gamma\gamma}$ and the dark matter density profile

To constrain dark matter distribution in inner Galaxy, we implement spherically symmetric generalized NFW profiles

$$\rho_{\rm DM}(r) = \rho_{\rm s}(r/r_{\rm s})^{-\alpha}(1 + r/r_{\rm s})^{-3+\alpha}, \qquad (5)$$

where $r_{\rm s}$ restricted in the range $10 - 35$ kpc is the scale radius (Iocco et al. 2011) and α is the inner slope for the NFW profile (it is found in the N-body simulations that $0.9 < \alpha < 1.2$, however the baryon compression
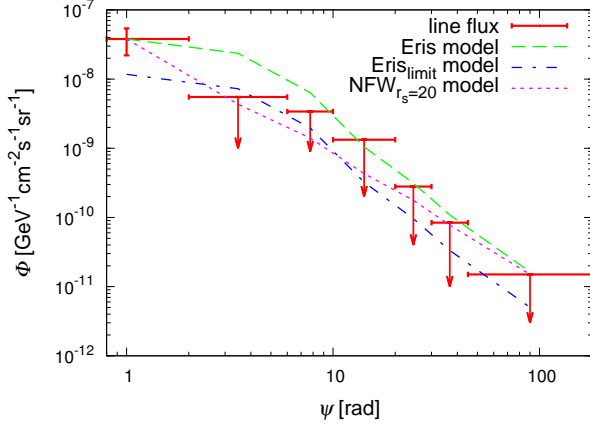
FIG. 3.— The annihilation line flux expected in the theoretical models vs. the current 130 GeV line data. See the text for details.
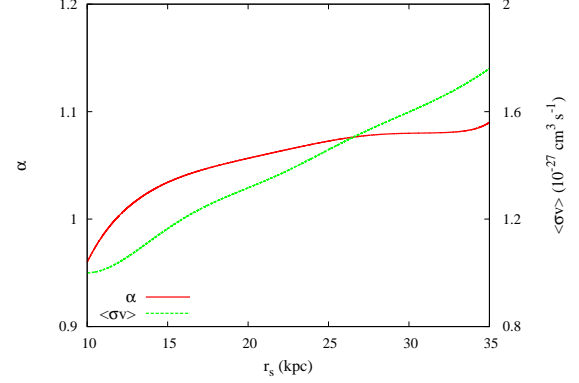

FIG. 4.— The 95% confidence level lower (upper) limit on the generalized NFW distribution parameter α ($\langle\sigma v\rangle_{\chi\chi\to\gamma\gamma}$) set by current 130 GeV line data for $\rho_0 = 0.4$ GeV cm^{-3}. Following Iocco et al. (2011), r_s is restricted within the range $10-35$ kpc.

may give rise to $\alpha \sim 1.7$). One main reason for adopting the generalized NFW profiles is that they can reproduce the three types of dark halo profiles presented in Maccio et al. (2012). The normalization of the DM profile is set by the local DM density, i.e., $\rho_0 \equiv \rho_{\rm DM}(R_\odot)$ and $\rho_{\rm s} = \rho_0(r_\odot/r_{\rm s})^\alpha(1 + r_\odot/r_{\rm s})^{3-\alpha}$, where $R_\odot \approx 8.5$ kpc is the distance from the Sun to the Galactic center. The fiducial interval $\rho_0 = 0.4 \pm 0.1$ GeV cm^{-3} is adopted in line with recent astrophysical measurements (Salucci et al. 2010). The γ-ray flux produced by DM annihilation can be written as

$$\Phi(\Delta\Omega, E_\gamma) = \frac{1}{4\pi} \times \frac{\langle\sigma v\rangle_{\chi\chi\to\gamma\gamma}}{2m_\chi^2} \frac{{\rm d}N_\gamma}{{\rm d}E_\gamma} \times \bar{J}(\Delta\Omega)\Delta\Omega, \quad (6)$$

where m_χ is the mass of DM particles and ${\rm d}N_\gamma/{\rm d}E_\gamma = 2\delta(E_\gamma - m_\chi)$ is the differential energy spectrum of γ-rays. The astrophysical factor ($\bar{J}$) is defined as

$$\bar{J}(\Delta\Omega) = \frac{1}{\Delta\Omega} \int_{\Delta\Omega} {\rm d}\Omega \int_{\rm LOS} {\rm d}l\, \rho^2(r(l)), \quad (7)$$

where $r(l)$ is the distance to the center of the object which is a function of line of sight (LOS) distance l.

For region (a), there is a tentative gamma-ray line signal. If interpreted as dark matter particles annihilating into a pair of photons, the cross section of dark matter annihilation ($\langle\sigma v\rangle_{\chi\chi\to\gamma\gamma,{\rm a}}$) can be inferred with equation (6). For regions (b), (c), (d), (e), (f) and (g) we have the 95% confidence level upper limits of the line flux and then get the constraints on the annihilation cross section. As long as

$$\langle\sigma v\rangle_{\chi\chi\to\gamma\gamma,{\rm a}} \leq \min\{\langle\sigma v\rangle_{\chi\chi\to\gamma\gamma,{\rm b}},\ \langle\sigma v\rangle_{\chi\chi\to\gamma\gamma,{\rm c}},$$
$$\langle\sigma v\rangle_{\chi\chi\to\gamma\gamma,{\rm d}},\ \langle\sigma v\rangle_{\chi\chi\to\gamma\gamma,{\rm e}},$$
$$\langle\sigma v\rangle_{\chi\chi\to\gamma\gamma,{\rm f}},\ \langle\sigma v\rangle_{\chi\chi\to\gamma\gamma,{\rm g}}\}, \quad (8)$$

the Dark Matter profile is in agreement with the 130 GeV $\gamma-$ray line data. Such a fit to the current tentative 130 GeV $\gamma-$ray line data suggests that $\alpha \geq 1.17$ and $\langle\sigma v\rangle_{\chi\chi\to\gamma\gamma} \leq 7.5 \times 10^{-28}$ cm^3 s^{-1} for $r_{\rm s} = 20$ kpc and $\rho_0 = 0.4$ GeV cm^{-3} (see the dotted line in Fig.3).

To get more robust constraint, we adopt a combined likelihood analysis in all seven regions to constrain $\langle\sigma v\rangle_{\chi\chi\to\gamma\gamma}$ and α for $r_{\rm s}$ ranging from 10 kpc to 35 kpc. The method is similar to that described in Tsai et al.

(2013) and the combined likelihood is calculated as

$$L_c = \Pi L_i, \quad (9)$$

where L_i is the unbinned likelihood in the $i-$th region. The definition of the unbinned likelihood is similar to that in last section, but now the influence of $\langle\sigma v\rangle_{\chi\chi\to\gamma\gamma}$ as well as α should be taken into account. For such a purpose we modify the signal ratio f in Eq.(1) to $f = \Phi(\langle\sigma v\rangle_{\chi\chi\to\gamma\gamma}, \alpha)/\Phi_{\rm obs}$, where $\Phi(\langle\sigma v\rangle_{\chi\chi\to\gamma\gamma}, \alpha)$ is the flux predicted in the DM model (i.e., eq.(6)) with varying $\langle\sigma v\rangle_{\chi\chi\to\gamma\gamma}$ and α, and $\Phi_{\rm obs}$ is the observed gamma ray flux (i.e., the integration of J_γ in Fig.1 in the whole energy range). In our approach the profile likelihood technique is adopted (Rolke et al. 2005). To constrain $\langle\sigma v\rangle_{\chi\chi\to\gamma\gamma}$ we treat α as a nuisance parameter and vice versa. $\Delta\ln(L_c) = 1.35$ is adopted to get upper (lower) limit corresponding to a coverage probability of 95%. In this work we do not constrain ρ_0 (or alternatively $\rho_{\rm s}$) since it couples with the annihilation cross section, i.e., $\langle\sigma v\rangle_{\chi\chi\to\gamma\gamma} \propto 1/\rho_0^2$. Our general 95% confidence level lower (upper) limit on α ($\langle\sigma v\rangle_{\chi\chi\to\gamma\gamma}$) as a function of $r_{\rm s}$ is presented in Fig.4. For $r_{\rm s} = 20$ kpc and $\rho_0 = 0.4$ GeV cm^{-3}, the 95% confidence level constraints are $\alpha \geq 1.06$ and $\langle\sigma v\rangle_{\chi\chi\to\gamma\gamma} \leq 1.3 \times 10^{-27}$ cm^3 s^{-1}, respectively. The required $\langle\sigma v\rangle_{\chi\chi\to\gamma\gamma}$ is consistent with the constraints set by the non-detection of a reliable signal in dwarf galaxies, diffuse Galactic halo and Galaxy Clusters (Strigari 2012; Bringman & Weniger 2012). Even for $r_{\rm s} = 10$ kpc, the smallest value suggested in Iocco et al. (2011), $\alpha \geq 0.96$ is needed and hence the HFR dark matter profile suggested in Maccio et al. (2012) is disfavored, implying that the baryonic processes that can considerably flatten the central dark matter distribution might not play an important role in the evolution of the Milky Way.

In Eris, a very recent high-resolution cosmological hydrodynamics simulation of a realistic Milky-Way-analog disk galaxy, the dark matter density profile within ~ 1 kpc is found to be very flat and the peak of the dark matter density profile is $\sim$ a few 100 pc away from the Galactic centre (Kuhlen et al. 2013). It is interesting to check whether the specific cored dark matter distribution found in Eris is consistent with the current line data or not. The fits to the data are shown in Fig.3. The dashed line represents the best fit. In region (b)

the divergency between the model and the data is by a factor of > 4. The dash-dotted line (i.e., the so-called Eris$_{\text{limit}}$ model) represents the case that the predicted flux of Eris model in region (a) has been normalized to a flux $\approx 1.17 \times 10^{-8}$ cm^{-2}s^{-1}sr^{-1}, i.e., the 95% confidence level lower limit of the line signal. In such a fit, the model predicted line flux in region (b) is still above the upper limit. We thus conclude that the Eris model has some tension with the line data.

3. SUMMARY

In the very inner region of the Galaxy, the dark matter abundance is much less than the normal matter, hence current micro-lensing and Galactic rotation curve data can not directly constrain the dark matter density distribution. The numerical simulations in principle can solve such a problem. However, our current knowledge of the history of the Galaxy is very limited and the complicated physical processes being able to shape the dark matter distribution are hard to fully address. That's why so far the distribution of dark matter in the very inner region of the Galaxy is still in heavy debate (e.g., Gnedin et al. 2004; Maccio et al. 2012; Pontzen & Governato 2012; Kuhlen et al. 2013). Recently several groups have identified tentative 130 GeV $\gamma-$ray line which might be due to the annihilation of dark matter particles in the inner Galaxy. In this work we adopt the hypothesis that these signals are due to dark matter annihilation and use this hypothesis to examine which DM profile is consistent with the line. Our finding is that at the 95% confidence level, the dark matter density profile towards the center should be not shallower than $r^{-1.06}$ (for the generalized NFW profile with $r_{\text{s}} = 20$ kpc) and the dark matter annihilation cross section should be smaller than $\langle \sigma v \rangle_{\chi\chi \to \gamma\gamma} = 1.3 \times 10^{-27}$ cm^3 s^{-1}($\rho_0/0.4$ GeV cm^{-3})$^{-2}$ (see Fig.4). Such a density profile is in agreement with that found in some N-body simulations and the baryon compression effect might play a role. The dissipative baryonic processes that are able to considerably flatten dark matter profiles seems to not play important roles in our Galaxy, implying that the formation and evolution of Milky Way may not follow a prototypical spiral galaxy. Finally we'd like to caution that the tentative 130 GeV $\gamma-$ray line has not been officially confirmed by the Fermi collaboration yet. Whether our constraints on the dark matter distribution in very inner Galaxy and on the corresponding annihilation cross section are robust or not will be directly tested by the upcoming pass 8 data of Fermi LAT, in which the amount of usual data at energies greater than 10 GeV is expected to be boosted by some 60% (Bloom et al. 2012).

REFERENCES

Ackermann, M. *et. al.*, 2012, Phys. Rev. D, 86, 022002 (arXiv:1205.2739)

Bloom, E., et al. 2012, 2012 Fermi Symposium proceedings - eConf C121028 (arXiv: 1303.2733)

Blumenthal, G. R., Faber, S. M., Flores, R., & Primack, J. R. 1986, ApJ, 301, 27

Bringmann, T., Huang, X., Ibarra, A., Vogl, S., & Weniger, C. 2012, J. Cos. Astropart. Phys. 07, 054

Bringmann, T., & Weniger, C. 2012, Dark Universe, 1, 194

Buckley, M. R. & Hooper, D. arXiv:1205.6811

Einasto, J. 1965, Trudy Astrofizicheskogo Instituta Alma-Ata. 5, 87

El-Zant, A., Shlosman, I., & Hoffman, Y. 2001, ApJ, 560, 636

Feng, L., Yuan, Q. Li, X. & Fan, Y. Z. 2013, Phys. Lett. B., 720, 1 (arXiv:1206.4758)

Gnedin, O. Y., Kravtsov, A. V., Klypin, A. A., & Nagai, D. 2004, ApJ, 616, 16

Geringer-Sameth, A. & Koushiappas, S., 2012, Phys. Rev. D 86, 021302

Huang, X. Y., Yuan, Q., Yin, P. F., Bi, X. J., & Chen, X. L. 2012, J. Cos. Astropart. Phys. 11, 048

Iocco, F., Pato, M., Bertonea, G., & Jetzerb, P. 2011, JCAP, 11, 029

Kuhlen, M., Guedes, J., Pillepich, A., Madau, P., & Mayer, L. 2013, ApJ in press (arXiv:1208.4844)

Maccio, A. V., et al. 2012, ApJ, 744, L9

Mashchenko, S., Couchman, H. M. P., & Wadsley, J. 2006, Nature, 442, 539

Mo, H. J., & Mao, S. 2004, MNRAS, 353, 829

Navarro, J. F., Eke, V. R., & Frenk, C. S. 1996, MNRAS, 283, L72

Navarro, J. F., Frenk C. S., & White, S. D. M. 1997, ApJ, 490, 493

Ogiya, G. & Mori, M. 2011, ApJ, 736, L2

Pontzen, A. & Governato, F. 2012, MNRAS 421, 3464

Rolke, W., Lopez, A. & Conrad, J. 2005, Nucl.Instrum.Meth., A551, 493

Sofue, Y. 2012, PASJ, 64, 75

Springel, V., Wang, J., & Vogelsberger, M., et al. 2008, MNRAS, 391, 1685

Salucci, P., Nesti, F., Gentile, G., & Martins, C. 2010, A&A, 523, 83

Strigari, L., arXiv:1211.7090

Su, M. & Finkbeiner, D. P. arXiv:1206.1616

Tempel, E., Hektor, A. & Raidal, M. 2012, JCAP, 09, 032 (arXiv:1205.1045)

Tsai, Y. S., Yuan, Q., & Huang, X. Y. 2013, arXiv:1212.3990

Weniger, C. 2012, J. Cos. Astropart. Phys. 08, 007

White, S. D. M., & Rees, M. J. 1978, MNRAS, 183, 341

Yang, R. Z., Yuan, Q., Feng, L., Fan, Y. Z., & Chang. J., 2012, Phys. Lett. B., 715, 285 (arXiv:1207.1621)